Hindawi Publishing Corporation
EURASIP Journal on Wireless Communications and Networking
Volume 2010, Article ID 956721, 14 pages
doi:10.1155/2010/956721

Research Article

Impact of Antenna Correlation on a New Dual-Hop MIMO AF Relaying Model

Gayan Amarasuriya, Chintha Tellambura, and Masoud Ardakani

Department of Electrical and Computer Engineering, University of Alberta, Edmonton, AB, Canada T6G 2V4

Correspondence should be addressed to Chintha Tellambura, chintha@ece.ualberta.ca

Received 24 November 2009; Revised 23 March 2010; Accepted 25 April 2010

Academic Editor: Claude Oestges

A novel system model is proposed for the dual-hop multiple-input multiple-output amplify-andforward relay networks, and the impact of antenna correlation on the performance is studied. For a semiarbitrary correlated source-relay channel and an arbitrary correlated relay-destination channel, the complementary cumulative distribution function (CCDF) and the moment-generating function (MGF) approximations of the end-to-end signal-to-noise ratio (SNR) are derived. The outage probability, the average symbol error rate (SER), and the ergodic capacity approximations are also derived. Two special cases are treated explicitly: (1) dual-antenna relay and multiple-antenna destination and (2) uncorrelated antennas at the relay and correlated antennas at the destination. For the first case, the CCDF, the MGF and the average SER of an upper bound of the end-to-end SNR are derived in closed-form. For the second case, the CCDF, the MGF, the average SER, and the moments of SNR are derived in closed-form; as well, the high SNR approximations for the outage probability and the average SER are derived, and the diversity gain and coding gain are developed. Extensive numerical results and Monte Carlo simulation results are presented to verify the analytical results and to quantify the detrimental impact of antenna correlations on the system performance.

1. Introduction

Cooperative relay networks have been the focus of a flurry of research activities and standard deployment [1–5]. The use of multiple antennas at the source, relay, and/or destination of relay networks offers significant performance gains [6–15]. Such cooperative multiple-input multiple-output (MIMO) relaying opens up the possibility of deploying diversity transmission techniques such as beamforming, maximal ratio transmission (MRT), maximal ratio combining (MRC), and transmit antenna selection (TAS) strategies [10–12, 15]. In this paper, a suboptimal yet a simple and efficient system model, which achieves a better trade-off among the hardware cost, complexity, and the performance, is proposed and analyzed for dual-hop MIMO amplify-and-forward (AF) relay networks.

Prior Related Research. The prior work can be divided into two broad categories. The first category deals with multiple-antenna terminals (source, relay, and destination) [6, 10–17]. The second category considers single-antenna terminals only [4, 5, 18–21].

Single-antenna AF relaying over two hops with source and destination using multiple antennas is analyzed in [10, 11, 13]. In these works, beamforming or MRT and MRC technologies are considered. The difference between [11] and [13] is that the former considers independent Rayleigh fading whereas the latter considers independent Nakagami-m fading. In particular, [10] extends [13] to study the effect of antenna correlation at the source and destination. Moreover, in [12], the performance in independent Rayleigh fading is derived for a system, where the source uses TAS and the destination, MRC.

References [6, 15] analyze the performance of dual-hop multibranch cooperative systems with decode-and-forward (DF) relays equipped with multiple receive antennas and a single transmit antenna. However, the source and the destination are single-antenna terminals. In [6], the performance metrics are derived by considering threshold-based MRC and threshold-based selection diversity combining at the

relay. Moreover, [15] extends [6] by employing distributed beamforming to achieve improved capacity gains.

In [14, 16, 17], the performance of single-relay system, where the source, the relay, and the destination terminals are equipped with multiple transmit/receive antennas, is analyzed. All these works employ space time block codes. The analysis in [14] considers both DF and AF relaying strategies. In [16], the performance analysis employs random matrix theory. Reference [17] derives the exact outage probability in closed form.

For the sake of completeness, we briefly mention some prior research of the second category dealing with single-antenna two-hop AF relay networks. Their performance over Rayleigh fading is analyzed in [4, 5]. The performance bounds for the multibranch case of such networks over Nakagami-m fading are derived in [18]. Reference [19] derives their performance over nonidentical Nakagami-m fading links. The performance bounds of such networks over generalized Gamma fading channels and nonidentical Weibull fading channels are derived in [20, 22]. In [21], the exact expressions and lower bounds for mixed Rayleigh and Rician fading channels are derived.

Motivation. Although the dual-hop MIMO relay models in [10–12, 15] provide significant performance gains over single-antenna relaying [4, 5, 18–20], the following issues may arise in practical network deployments of such networks. In the emerging cellular dual-hop relay networks, employing multiple antennas at the mobile stations (MS) is strictly limited due to power and space constraints. However, there are no such constrains at the base stations (BS). On the other hand, the hardware cost and complexity associated with the relay should be low compared to a traditional BS. Although relaying can be performed by an MS as well, in this work, an infrastructure (fixed) relay [7] is considered. Such a relay can employ multiple antennas.

In this paper, we consider a practical scenario where a single-antenna MS communicates with a multiple-antenna BS via a fixed relay equipped with multiple antennas. This particular setup is shown in Figure 1. The relay uses selection diversity combining (SDC) for signal reception and uses one transmit antenna for forwarding the amplified signal. Although several other antenna setups are possible for the relay, we focus on this setup for several reasons. First, alternatives such as MRC are more costly; if the relay employs MRC reception, a separate receiver chain is required for each receive antenna, and this requirement increases the cost and complexity. Second, a single transmit antenna at the relay keeps the cost comparable to that of a single antenna relay, which requires only one transmit chain. Although this particular transmit/receive strategy adopted at the relay may not be optimal, it is designed to gain MIMO diversity benefits yet keep the costs/complexity at the relay as low as possible. Finally, from a theoretical point of view, there is no difficulty in analyzing other antenna configurations at the relay, but space limitations prevent us from doing so. The proposed system model may thus readily be used for emerging cellular networks with MIMO relaying, where the use of multiple antennas in a BS is reasonable; however the use of multiple antennas at MS may be strictly limited due to the terminal size and power constraints.

Our Contribution. Although MIMO techniques achieve diversity/SNR gains, these gains decrease when there is spatial correlation among the signals received by antenna elements. Therefore, the performance losses due to antenna correlations must be quantified. In this paper, in particularly, we consider the impact of spatial (antenna) correlation on our proposed dual-hop MIMO AF relay network (Figure 1). To the best of our knowledge, the proposed network setup has not been analyzed before, and the differences between our work and [6, 10] are as follows. The setup in [10] studies a multiple-antenna source and single-antenna relay. Moreover, in [10], MRT and MRC are employed at the source and destination whereas our setup employs SDC and MRC at the relay and destination, respectively. Although reference [6] considers a relay identical to ours, the destination is a single-antenna terminal. The relaying strategy in [6] is DF whereas AF relaying is considered here. Further, [6] considers independent fading whereas our work treats consider correlated fading.

In our work, for a semiarbitrary correlated source-relay channel and arbitrary correlated relay-destination channel, we derive integral expressions for the complementary cumulative distribution function (CCDF) and the moment-generating function (MGF) of the end-to-end signal-to-noise ratio (SNR). The numerically efficient Gauss-Laguerre quadrature rule [23] is employed to evaluate the integrals. The outage probability, the average symbol error rate (SER), and the ergodic capacity expressions are also derived. Closed-form expressions are derived for the performance of two special cases of antenna correlation: (1) dual-antenna relay and multiple-antenna destination and (2) uncorrelated antennas at the relay and correlated antennas at the destination. We develop closed-form expressions for the CCDF and the MGF of an upper bound of the SNR for the first case. The average SER is evaluated by using the Gauss-Chebyshev quadrature rule [23]. Exact closed-form expressions are derived for the CCDF, the MGF, the average SER, and the moments of SNR of the second case. In particular, for the second case, the high SNR approximations for the outage probability and the average SER are derived and used to obtain valuable insights such as the diversity and the coding gains. Numerical and Monte Carlo simulation results are provided to analyze the system performance, obtain valuable insights, and validate our analysis. The insights provided by our analysis may well be used for designing of MIMO relay networks.

The rest of this paper is organized as follows. Section 2 presents the system and the channel model. In Section 3, the performance analysis is presented. Section 4 contains the numerical and simulation results. Section 5 concludes the paper, and the proofs are annexed.

Notations. $\mathcal{K}_\nu(z)$ is the *Modified Bessel function of the second kind of order* ν [23, 9.6]. ${}_2\mathcal{F}_1(\alpha,\beta;\gamma;z)$ is the *Gauss Hypergeometric function* [23, 15.1]. $\mathcal{Q}(z)$ denotes the *Gaussian Q-function* [23, 26.2.3]. $\mathcal{Q}_m(a,b)$ is the *mth-order Marcum Q-function* [24, equation (1)]. For the sake of brevity, we

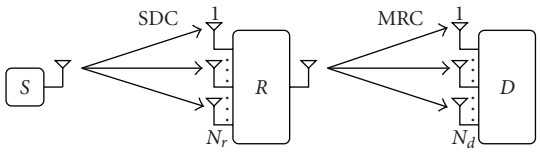

Figure 1: System model: dual-hop MIMO relaying.

write $\mathcal{Q}(a,b)$ to denote $\mathcal{Q}_1(a,b)$. $I_m(z)$ is the *mth-order Modified Bessel function of the first kind* [23, 9.6.3]. $E_i(z)$ is the *Exponential integral function* [25, 8.211.1]. $\mathcal{E}_\Lambda\{z\}$ denotes the *expected value of* z over Λ. $\|\mathbf{Z}\|_F$ and $(\mathbf{Z})^H$ are the *Frobenius norm* and *conjugate transpose* of $\mathbf{Z}$.

2. System and Channel Model

We consider the dual-hop relay network in Figure 1. The single-antenna source (S) communicates with the destination (D) having $N_d \geq 1$ antennas via an AF relay (R). The relay has $N_r \geq 1$ receive antennas and uses only one antenna among them for forwarding. (Although TAS can be used at the relay for the second time slot, it provides diversity gains only when $N_r > N_d$ despite the additional CSI feedback requirement (see Remark 1 in Section 3). However, in practice, $N_r > N_d$ is unlikely even since the relays should usually be more cost/complexity effective than BS.) Half-duplex transmission is assumed. Since we consider a MIMO-enabled infrastructure relay, which is used primarily for extending the network coverage, the direct channel between S and D, which is far apart, is not considered assuming heavy shadowing and path loses. Cooperation occurs in two timeslots. In the first timeslot, the source transmits to the relay. In the second timeslot, the relay forwards an amplified version of the source signal to the destination. The relay and destination employ SDC and MRC receptions, respectively. Perfect channel state information is assumed to be available at the relay and destination.

2.1. Source-to-Relay Channel Model. An arbitrary correlation model for the source-to-relay ($S \rightarrow R$) channel appears to be analytically intractable for dual-hop AF relay networks. We instead consider the semiarbitrary correlation model. (The use of the semiarbitrary correlation model simplifies the N_r-fold numerical integration [26] in evaluating the CCDF of the SDC output SNR for the $S \rightarrow R$ channel into a single integral [27] and thereby enables the efficient computation of distribution functions of the end-to-end SNR of dual-hop AF relaying.) In other words, the $S \rightarrow R$ single-input multiple-output (SIMO) channel is a semiarbitrary correlated [27] flat Rayleigh fading channel. The $S \rightarrow R$ channel vector is given by $\mathbf{\Psi}_R^{1/2}\mathbf{h}_{sr}$, where $\mathbf{\Psi}_R$ is the $N_r \times N_r$ covariance matrix at the relay, and $\mathbf{h}_{sr}$ is an $N_r \times 1$ vector with independent Rayleigh fading entries. The (p,q)th element of $\mathbf{\Psi}_R$ is given by [28, 8.1.5]

$$\mathbf{\Psi}_R^{p,q} = \begin{cases} \rho_p \rho_q, & p \neq q \\ 1, & p = q \end{cases} \quad \text{where } 0 \leq \left(\rho_p, \rho_q\right) \leq 1. \tag{1}$$

Thus, $\mathbf{\Psi}_R^{p,q}$ can be parameterized by a $1 \times N_r$ vector $\overline{\rho}$ with the pth element ρ_p.

2.2. Relay-to-Destination Channel Model. The relay-to-destination ($R \rightarrow D$) SIMO channel is an arbitrary correlated [29] flat Rayleigh fading channel. In this case, the $R \rightarrow D$ channel vector is given by $\mathbf{\Psi}_D^{1/2}\mathbf{h}_{rd}$, where $\mathbf{\Psi}_D$ is the covariance matrix at the destination, and $\mathbf{h}_{rd}$ is an $N_d \times 1$ vector with independent Rayleigh fading entries. $\mathbf{\Psi}_D$ is constructed according to a practical channel model [30, 31] with the (p,q)th element given by

$$\mathbf{\Psi}_D^{p,q} = e^{-j2\pi(p-q)l_d\cos(\overline{\theta}_d)} e^{-(1/2)(2\pi(p-q)l_d\sin(\overline{\theta}_d)\sigma_d)^2}, \tag{2}$$

where l_d is the relative antenna spacing between adjacent antennas (measured in number of wavelengths) of the linear array of antennas at the destination, $\overline{\theta}_d$ is the mean angle of arrival, and σ_d^2 is the destination angular spread. The actual angle of arrival is given by $\underline{\theta}_d = \overline{\theta}_d + \widehat{\theta}_d$ with $\widehat{\theta}_d \sim \mathcal{N}(0, \sigma_d^2)$. Such a correlation model may arise in practice in uniform linear antenna arrays, and this model appears to be adequate to describe a real-world scattering environment [30].

2.3. The End-to-End SNR. The received signal vector at the relay can be written as

$$\mathbf{y_r} = \sqrt{P_1}\mathbf{\Psi}_R^{1/2}\mathbf{h}_{sr}x + \mathbf{n_r}, \tag{3}$$

where P_1 is the transmit power; x is the transmitted symbol satisfying $\mathcal{E}\{|x|^2\} = 1$; $\mathbf{n_r}$ is the additive white Gaussian noise (AWGN) vector with mean zero and variance N_o. The relay employs SDC to obtain the scalar signal as

$$y_r = \sqrt{P_1}h_{sr}^I x + n_r, \tag{4}$$

where $|h_{sr}^I| = \max_{1\leq i\leq N_r}|h_{sr}^i|$ and $\{h_{sr}^i\}_{i=1}^{N_r}$ are the elements of $\mathbf{\Psi}_R^{1/2}\mathbf{h}_{sr}$ and n_r is the AWGN at the Ith antenna. In the second timeslot, the signal y_r is amplified with the gain G and forwarded to the destination. The received signal at the destination can be written as

$$y_d = \mathbf{w}^H\left(\sqrt{P_2}\mathbf{\Psi}_D^{1/2}\mathbf{h}_{rd}Gy_r + \mathbf{n}_d\right), \tag{5}$$

where P_2 is the relay transmit power factor, $\mathbf{n}_d$ is the $N_d \times 1$ AWGN vector satisfying $\mathcal{E}\{\mathbf{n}_d\mathbf{n}_d^H\} = N_o\mathbf{I}_{N_r}$, and $\mathbf{w}^H$ is the receive weight vector for MRC operation [32] given by $\mathbf{w} = \mathbf{\Psi}_D^{1/2}\mathbf{h}_{rd}/\|\mathbf{\Psi}_D^{1/2}\mathbf{h}_{rd}\|_F$. Next, we expand (5) to obtain the following model for the received signal at the destination:

$$\begin{aligned} y_d = {} & \sqrt{P_1P_2}G\|\mathbf{\Psi}_D^{1/2}\mathbf{h}_{rd}\|_F h_{sr}^I x + \sqrt{P_2}G\|\mathbf{\Psi}_D^{1/2}\mathbf{h}_{rd}\|_F n_r \\ & + \left(\mathbf{\Psi}_D^{1/2}\mathbf{h}_{rd}\right)^H\mathbf{n}_d. \end{aligned} \tag{6}$$

By using (6), the resulting SNR can be obtained as

$$\gamma_{\text{eq}} = \frac{\left(P_1\left|h_{sr}^I\right|^2/N_o\right)\left(P_2\|\mathbf{\Psi}_D^{1/2}\mathbf{h}_{rd}\|_F^2/N_o\right)}{P_2\|\mathbf{\Psi}_D^{1/2}\mathbf{h}_{rd}\|_F^2/N_o + 1/G^2N_o}. \tag{7}$$

The gains of practical channel state information-(CSI-) assisted relays can be defined as in [1, 4]. Thus, by

substituting $G = \sqrt{1/(P_1|h_{sr}^I|^2 + N_o)}$ into (7), the SNR of the dual-hop system with the practical CSI-assisted relay can be written as follows:

$$\gamma_{\text{eq}} = \frac{\gamma_1\gamma_2}{\gamma_1 + \gamma_2 + 1}, \tag{8}$$

where $\gamma_1 = P_1|h_{sr}^I|^2/N_o$ is the instantaneous SNR of the SDC output at the relay in semiarbitrary correlated Rayleigh fading, and $\gamma_2 = P_2\|\mathbf{\Psi}_D^{1/2}\mathbf{h}_{rd}\|_F^2/N_o$ is the instantaneous SNR of the MRC output at the destination over arbitrary correlated Rayleigh fading. We also define $\overline{\gamma}_1 = \mathcal{E}\{\gamma_1\}$ and $\overline{\gamma}_2 = \mathcal{E}\{\gamma_2\}$ as the average of γ_1 and γ_2, respectively.

We can also consider ideal CSI-assisted relays that invert the $S \to R$ channel regardless of its fading state [4]. For this case, the relay gain is given by $G = \sqrt{1/P_1|h_{sr}^I|^2}$, and the SNR $\gamma_{\text{eq,ideal}}$ is given by [4]

$$\gamma_{\text{eq}} \le \gamma_{\text{eq,ideal}} = \frac{\gamma_1\gamma_2}{\gamma_1 + \gamma_2}. \tag{9}$$

Moreover, the γ_{eq} can be upper bounded as [5, 18]

$$\gamma_{\text{eq}} \le \gamma_{\text{eq,ideal}} \le \gamma_{\text{eq}}^{\text{ub}} = \min(\gamma_1, \gamma_2). \tag{10}$$

3. Performance Analysis

This section presents a comprehensive performance analysis of our proposed MIMO relay network model by taking into account the spatial correlation of antenna elements at the MIMO-enabled terminals. The CCDF and the MGF of the end-to-end SNR γ_{eq} are derived and used to obtain accurate closed-form approximations the outage probability, the average symbol error rate (SER), and the ergodic capacity.

3.1. Statistical Characterization of the End-to-End SNR. An accurate closed-form approximation for the CCDF of the end-to-end SNR in (8) can be derived as (Appendix A)

$$\begin{aligned}\overline{F}_{\gamma_{\text{eq}}}(x) &\approx \frac{1}{\Delta(\mathbf{\Psi}_D)}\sum_{j=1}^{N_d}(-1)^{N_d+j}\lambda_j^{N_d-1}\Delta_{N_d,j}(A(\mathbf{\Psi}_D)) \\ &\quad\times e^{-x/\overline{\gamma}_2\lambda_j}\left(1 - \sum_{p=1}^{L}\sum_{q=1}^{L} w_p w_q \right. \\ &\quad\left.\times \prod_{k=1}^{N_r}\left[1 - \mathcal{Q}\left(\sqrt{\frac{2\rho_k t_q}{1-\rho_k}}, \sqrt{\frac{2x\left(x + \overline{\gamma}_2\lambda_j y_p + 1\right)}{\overline{\gamma}_1\overline{\gamma}_2\lambda_j(1-\rho_k)y_p}}\right)\right]\right),\end{aligned} \tag{11}$$

where $\lambda_1 > \cdots > \lambda_{N_d}$ are the eigenvalues of $\mathbf{\Psi}_D$, $\Delta(\mathbf{\Psi}_D)$ is the determinant of the Vandermonde matrix of the eigenvalues of $\mathbf{\Psi}_D$, and $\Delta_{N_d,j}(\mathcal{M})$ is the determinant of the matrix $\mathcal{M}$ with N_dth row and jth column removed. The (i, j)th element of $A(\mathcal{M})$ is given by $A(\mathcal{M})_{i,j} = v_j^{i-1}$ where v denotes the eigenvalues of $\mathcal{M}$. Further, $\{w_p, w_q\}_{p=1,q=1}^{L}$ and $\{y_p, t_q\}_{p=1,q=1}^{L}$ are the weights and the nodes of the Gauss-Laguerre quadrature rule, respectively. The nodes (y_p, t_q) and weights (w_p, w_q) can be efficiently computed by using the approach proposed in [33]. Moreover, L is the number of terms used for the Gauss-Laguerre quadrature rule.

The MGF of the end-to-end SNR is a useful statistic which can be used to analyze a wide range of performance metrics. The MGF of γ_{eq} can accurately be approximated as follows (Appendix A):

$$\begin{aligned}M_{\gamma_{\text{eq}}}(s) &\approx 1 - \frac{1}{\Delta(\mathbf{\Psi}_D)}\sum_{j=1}^{N_d}(-1)^{N_d+j}\lambda_j^{N_d}\Delta_{N_d,j}(A(\mathbf{\Psi}_D)) \\ &\quad\times \frac{s}{\lambda_j s + 1/\overline{\gamma}_2}\left(1 - \sum_{p=1}^{L}\sum_{q=1}^{L}\sum_{r=1}^{L} w_p w_q w_r \right. \\ &\quad\left.\times \prod_{k=1}^{N_r}\left[1 - \mathcal{Q}\left(\sqrt{\alpha_{k,r}}, \sqrt{\beta_{k,p,q}}\right)\right]\right),\end{aligned} \tag{12}$$

where $\alpha_{k,r} = 2\rho_k t_r/(1-\rho_k)$ and $\beta_{k,p,q} = 2\overline{z}_q(\overline{\gamma}_2\lambda_j z_q + (1 + \overline{\gamma}_2\lambda_j y_p)(1 + \overline{\gamma}_2\lambda_j s))/\overline{\gamma}_1(1 + \overline{\gamma}_2\lambda_j s)^2(1-\rho_k)y_p$.

3.2. Outage Probability. The outage probability is the probability that the instantaneous SNR γ_{eq} falls below a predefined SNR threshold γ_{th}. Thus, the outage probability P_{out} can readily be obtained by using (11) as follows:

$$P_{\text{out}} = \Pr\left(\gamma_{\text{eq}} \le \gamma_{\text{th}}\right) = 1 - \overline{F}_{\gamma_{\text{eq}}}(\gamma_{\text{th}}). \tag{13}$$

3.3. Average Symbol Error Rate. The average SER is an important performance metric of wireless networks. The conditional error probability (CEP) of the coherent binary frequency-shift keying (C-BFSK) and M-ary pulse amplitude modulation (PAM) is given as $P_e \mid \gamma = a\mathcal{Q}(\sqrt{b\gamma})$ [32], where a and b are constants dependent on the modulation scheme. For example, the cases $(a = 1, b = 2)$ and $(a = 1, b = 1)$ yield the exact bit error rate of the coherent binary phase-shift keying (BPSK) and C-BFSK, respectively. Further, the SER of M-ary PAM is given by $(a = 2(M-1)/M)$ and $(b = 6\log_2 M/M^2 - 1)$ [32]. An accurate closed form average SER approximation can be derived by integrating $P_e \mid \gamma$ over the PDF of the SNR γ_{eq} as follows (Appendix B):

$$\begin{aligned}\overline{P}_e &\approx \frac{a}{2} - \frac{a}{2\Delta(\mathbf{\Psi}_D)}\sqrt{\frac{b}{2}}\sum_{j=1}^{N_d}(-1)^{N_d+j}\lambda_j^{N_d-1}\Delta_{N_d,j}(A(\mathbf{\Psi}_D)) \\ &\quad\times \sqrt{\frac{2}{b + 2/\overline{\gamma}_2\lambda_j}}\left(1 - \frac{1}{\sqrt{\pi}}\sum_{p=1}^{L}\sum_{q=1}^{L}\sum_{r=1}^{L} w_p w_q w_r z_q^{-1/2} \right. \\ &\quad\left.\times \prod_{k=1}^{N_r}\left[1 - \mathcal{Q}\left(\sqrt{\alpha_{k,r}}, \sqrt{\zeta_{k,p,q}}\right)\right]\right),\end{aligned} \tag{14}$$

where $\alpha_{k,r} = 2\rho_k t_r/(1-\rho_k)$ and $\zeta_{k,p,q} = 4z_q(2z_q + (1 + \overline{\gamma}_2\lambda_j y_p)(2 + b\overline{\gamma}_2\lambda_j))/\overline{\gamma}_1(2 + b\overline{\gamma}_2\lambda_j)^2(1-\rho_k)y_p$.

3.4. Ergodic Capacity. The channel capacity is defined as the maximum data rate at which information can be transmitted across a noisy channel with arbitrary reliability. The ergodic capacity $C_{\gamma_{\text{eq}}}$ is defined as the expected value of the instantaneous maximum mutual information I between S and D. For a dual-hop cooperative relay system operating over two timeslots per burst, I is given by $I = (1/2)\log_2(1+\gamma_{\text{eq}})$ [1]. Then, the ergodic capacity can be expressed as $C_{\gamma_{\text{eq}}} = (1/2)\mathcal{E}\{\log_2(1+\gamma_{\text{eq}})\} = \int_0^\infty (\overline{F}_{\gamma_{\text{eq}}}(x)/2\log_e(2)(1+x))\mathrm{d}x$. By substituting (A.4) into $C_{\gamma_{\text{eq}}}$ and applying the Gauss-Laguerre quadrature rule, an approximation for $C_{\gamma_{\text{eq}}}$ in closed form is obtained as follows:

$$C_{\gamma_{\text{eq}}} \approx \frac{1}{2\log_e(2)\Delta(\boldsymbol{\Psi}_D)} \sum_{j=1}^{N_d} (-1)^{N_d+j} \lambda_j^{N_d-1} \Delta_{N_d,j}(A(\boldsymbol{\Psi}_D)) \times \left(-e^{1/\overline{\gamma}_2\lambda_j} E_i\left(-\frac{1}{\overline{\gamma}_2\lambda_j}\right) - \sum_{p=1}^{L}\sum_{q=1}^{L}\sum_{r=1}^{L} w_p w_q w_r \times \left(z_q + \frac{1}{\overline{\gamma}_2\lambda_j}\right)^{-1} \prod_{k=1}^{N_r} \left[1 - \mathcal{Q}\left(\sqrt{\alpha_{k,r}}, \sqrt{\eta_{k,p,q}}\right)\right] \right), \tag{15}$$

where $\alpha_{k,r} = 2\rho_k t_r/(1-\rho_k)$ and $\eta_{k,p,q} = 2z_q(\overline{\gamma}_2\lambda_j(y_p+t_r)+1)/\overline{\gamma}_1(1-\rho_k)y_p$.

3.5. Special Cases. In this section, two special cases of our proposed system model are analyzed.

3.5.1. Two Receive Antennas at the Relay ($N_r = 2$). Consider the case where only two receive antennas are at the relay. This case may arise in practise due to the space limitations at the relay or due to the cost factor. In this section, the lower bounds for the outage probability and the average SER are derived in closed form by using the upper bound of the SNR $\gamma_{\text{eq}}^{\text{ub}}$ in (10).

The CCDF of $\gamma_{\text{eq}}^{\text{ub}}$ can be written as [34]

$$\overline{F}_{\gamma_{\text{eq}}^{\text{ub}}}(x) = \overline{F}_{\gamma_1}(x)\overline{F}_{\gamma_2}(x). \tag{16}$$

When $N_r = 2$, the CCDF of SDC in the equally correlated Rayleigh fading channels given in (A.2) reduces to the well-known result [35, 36]

$$\overline{F}_{\gamma_1}(x) = 2e^{-x/\overline{\gamma}_1}\mathcal{Q}\left(\sqrt{\frac{2x}{\overline{\gamma}_1(1-\rho^2)}}, \rho\sqrt{\frac{2x}{\overline{\gamma}_1(1-\rho^2)}}\right) - e^{-2x/\overline{\gamma}_1(1-\rho^2)} I_0\left(\frac{2\rho x}{\overline{\gamma}_1(1-\rho^2)}\right). \tag{17}$$

The CCDF of γ_2 can readily be obtained by using (A.3) and $\overline{F}_{\gamma_2} = 1 - \int_0^x f_{\gamma_1}(t)\mathrm{d}t$ as follows:

$$\overline{F}_{\gamma_2}(x) = \sum_{j=1}^{N_d} \frac{(-1)^{j+N_d}}{\Delta(\boldsymbol{\Psi}_D)} \lambda_j^{N_d-1} \Delta_{N_d,j}(A(\boldsymbol{\Psi}_D)) e^{-x/\overline{\gamma}_2\lambda_j}. \tag{18}$$

Then, the closed-form expression for the CCDF of $\gamma_{\text{eq}}^{\text{ub}}$ can be obtained by substituting (17) and (18) into (16) as follows:

$$\overline{F}_{\gamma_{\text{eq}}^{\text{ub}}}(x) = \frac{1}{\Delta(\boldsymbol{\Psi}_D)} \sum_{j=1}^{N_d} (-1)^{j+N_d} \lambda_j^{N_d-1} \Delta_{N_d,j}(A(\boldsymbol{\Psi}_D)) \times \left(2e^{-\mu x}\mathcal{Q}\left(\sqrt{\frac{2x}{\overline{\gamma}_1(1-\rho^2)}}, \rho\sqrt{\frac{2x}{\overline{\gamma}_1(1-\rho^2)}}\right) - e^{-\nu x} I_0\left(\frac{2\rho x}{\overline{\gamma}_1(1-\rho^2)}\right)\right), \tag{19}$$

where $\mu = (\overline{\gamma}_1 + \overline{\gamma}_2\lambda_j)/\overline{\gamma}_1\overline{\gamma}_2\lambda_j$ and $\nu = (\overline{\gamma}_1(1-\rho^2) + 2\overline{\gamma}_2\lambda_j)/\overline{\gamma}_1\overline{\gamma}_2\lambda_j(1-\rho^2)$.

The MGF of $\gamma_{\text{eq}}^{\text{ub}}$ can be derived in closed-form by substituting (19) into (A.5) as follows:

$$M_{\gamma_{\text{eq}}^{\text{ub}}}(s) = 1 - \frac{1}{\Delta(\boldsymbol{\Psi}_D)} \sum_{j=1}^{N_d} (-1)^{j+N_d} \lambda_j^{N_d-1} \Delta_{N_d,j}(A(\boldsymbol{\Psi}_D)) \times s\left(\frac{1}{s+\mu}\left(1 + \frac{(s+\mu+1/\overline{\gamma})}{\sqrt{(s+\mu+\varepsilon)^2 - \varsigma^2}}\right) - \frac{1}{\sqrt{(s+\nu)^2-\varsigma^2}}\right), \tag{20}$$

where $\varsigma = 2\rho/\overline{\gamma}_1(1-\rho^2)$ and $\varepsilon = (1+\rho^2)/\overline{\gamma}_1(1-\rho^2)$.

With the aid of (19), a lower bound of the outage probability can readily be computed as follows: $P_{\text{out}}^{\text{lb}} = 1 - \overline{F}_{\gamma_{\text{eq}}^{\text{ub}}}(\gamma_{\text{th}})$.

Next, we present an accurate and computationally efficient closed-form approximation for computing a lower bound for the average SER. The CEP of the coherent binary frequency-shift keying (C-BFSK) and M-ary PAM can be expressed in an alternative form [37] as $P_e \mid \gamma = a\mathcal{Q}(\sqrt{b\gamma}) = (a/\pi)\sqrt{(b/2)}\int_0^\infty (\exp(-\gamma(s^2+b/2))/(s^2+b/2))ds$. The average error rate can be obtained in the following form by averaging the alternative CEP expression over the PDF of $\gamma_{\text{eq}}^{\text{ub}}$ and manipulating it with the variable transformation $s^2 + b/2 = b/(x+1)$ [37]:

$$\overline{P}_e^{\text{lb}} = \frac{a}{\pi}\sqrt{\frac{b}{2}}\int_0^\infty \frac{M_{\gamma_{\text{eq}}^{\text{ub}}}(s^2+b/2)}{s^2+b/2}ds = \frac{a}{2\pi}\int_{-1}^{1} \frac{M_{\gamma_{\text{eq}}^{\text{ub}}}(b/(\gamma+1))}{\sqrt{1-\gamma^2}}d\gamma. \tag{21}$$

We use an accurate and computationally efficient method in [37] which uses the Gauss-Chebyshev quadrature rule [23] to obtain a very compact closed-form expression for (21):

$$\overline{P}_e^{\text{lb}} = \frac{a}{2N_p}\sum_{n=1}^{N_p} M_{\gamma_{\text{eq}}^{\text{ub}}}\left(\frac{b}{2}\sec^2(\theta_n)\right) + R_{N_p}, \tag{22}$$

where N_p is a positive integer, $\theta_n = (2n-1)\pi/4N_p$, and R_{N_p} is the remainder term. R_{N_p} becomes negligible as N_p increases

[37]. Thus, the lower bound of average SER can be obtained by substituting (20) into (22).

Moreover, for the CEP of the noncoherent binary frequency-shift keying (NC-BFSK) and differential BPSK (D-BPSK) is given in the form [32] $P_e \mid \gamma = ae^{-b\gamma}$, with $(a = 0.5, b = 1)$ and $(a = 0.5, b = 0.5)$ for D-BPSK and NC-BFSK, respectively. Now, the average SER of NC-BFSK and D-BPSK can be derived by substituting (19) into $\overline{P}_e^{\text{lb}} = a - ab\int_0^\infty \overline{F}_{\gamma_{\text{eq}}^{\text{ub}}}(x)e^{-bx}\mathrm{d}x$ as follows:

$$\overline{P}_e^{\text{lb}} = a - \frac{ab}{\Delta(\mathbf{\Psi}_D)}\sum_{j=1}^{N_d}(-1)^{j+N_d}\lambda_j^{N_d-1}\Delta_{N_d,j}(A(\mathbf{\Psi}_D)) \times\left(\frac{1+\varpi/\varrho}{b+\mu} - \frac{1}{\sqrt{(b+\nu)^2-\varsigma^2}}\right), \tag{23}$$

where $\varpi = b+(\overline{\gamma}_1+2\overline{\gamma}_2\lambda_j)/\overline{\gamma}_1\overline{\gamma}_2\lambda_j$ and $\varrho = \sqrt{(b+\varepsilon+\mu)^2-\varsigma^2}$.

3.5.2. Uncorrelated Antennas at the Relay ($\rho = 0$). When the antenna spacing at the relay is sufficiently large, the $S \to R$ channels experience independent Rayleigh fading. In this case, the CCDF of γ_{eq} can be obtained by substituting $\rho = 0$ in (A.4) and by using the identity of the Marcum-Q function, $\mathcal{Q}(0,x) = e^{-x^2/2}$, as follows (Appendix D):

$$\overline{F}_{\gamma_{\text{eq}}}(x) = \frac{2}{\Delta(\mathbf{\Psi}_D)}\sum_{j=1}^{N_d}\sum_{l=1}^{N_r}\binom{N_r}{l}(-1)^{j+l+N_d+1}\lambda_j^{N_d-1} \times\Delta_{Nd,j}(A(\mathbf{\Psi}_D))\sqrt{\frac{x(x+1)l}{\overline{\gamma}_1\overline{\gamma}_2\lambda_j}}e^{-x((\overline{\gamma}_1+\overline{\gamma}_2\lambda_j l)/\overline{\gamma}_1\overline{\gamma}_2\lambda_j)} \times\mathcal{K}_1\left(2\sqrt{\frac{x(x+1)l}{\overline{\gamma}_1\overline{\gamma}_2\lambda_j}}\right). \tag{24}$$

Let us consider an ideal CSI-assisted relay. For this case, the SNR $\gamma_{\text{eq,ideal}}$ is given in (9), and the CCDF of $\gamma_{\text{eq,ideal}}$ can be easily obtained with the aid of (24) as follows:

$$\overline{F}_{\gamma_{\text{eq,ideal}}}(x) = \frac{2}{\Delta(\mathbf{\Psi}_D)}\sum_{j=1}^{N_d}\sum_{l=1}^{N_r}\binom{N_r}{l}(-1)^{j+l+N_d+1}\lambda_j^{N_d-1} \times\Delta_{Nd,j}(A(\mathbf{\Psi}_D))\sqrt{\frac{l}{\overline{\gamma}_1\overline{\gamma}_2\lambda_j}}xe^{-x((\overline{\gamma}_1+\overline{\gamma}_2\lambda_j l)/\overline{\gamma}_1\overline{\gamma}_2\lambda_j)} \times\mathcal{K}_1\left(2x\sqrt{\frac{l}{\overline{\gamma}_1\overline{\gamma}_2\lambda_j}}\right). \tag{25}$$

The PDF of γ_{eq} and $\gamma_{\text{eq,ideal}}$ can easily be derived by differentiating (24) and (25) with respect to x and by using $x(\partial\mathcal{K}_\nu(x)/\partial x) + \nu\mathcal{K}_\nu(x) + x\mathcal{K}_{\nu-1}(x) = 0$ [38, 8.486.12]. However, for the sake of brevity, the PDF results are omitted.

A closed-form expression for the MGF of $\gamma_{\text{eq,ideal}}$ can be derived by substituting (A.4) into (A.5) as shown in Appendix E:

$$M_{\gamma_{\text{eq,ideal}}}(s) = 1 - \frac{64}{3\overline{\gamma}_1\overline{\gamma}_2\Delta(\mathbf{\Psi}_D)}\sum_{j=1}^{N_d}\sum_{l=1}^{N_r}\binom{N_r}{l}l(-1)^{j+l+N_d+1} \times\lambda_j^{N_d-2}\Delta_{Nd,j}(A(\mathbf{\Psi}_D)) \times\frac{s\,{}_2\mathcal{F}_1(3,3/2;5/2;(s+\psi-\varphi)/(s+\psi+\varphi))}{(s+\psi+\varphi)^3}, \tag{26}$$

where $\psi = (\overline{\gamma}_1+\overline{\gamma}_2\lambda_j l)/\overline{\gamma}_1\overline{\gamma}_2\lambda_j$ and $\varphi = 2\sqrt{l/\overline{\gamma}_1\overline{\gamma}_2\lambda_j}$.

By substituting (24) into (B.1), a closed-form expression for the average SER can be derived as follows (Appendix F):

$$\overline{P}_{e,\text{ideal}} = \frac{a}{2} - \frac{3a\pi}{\overline{\gamma}_1\overline{\gamma}_2\Delta(\mathbf{\Psi}_D)}\sqrt{\frac{b}{2}}\sum_{j=1}^{N_d}\sum_{l=1}^{N_r}\binom{N_r}{l}l(-1)^{j+l+N_d+1} \times\lambda_j^{N_d-2}\Delta_{Nd,j}(A(\mathbf{\Psi}_D)) \times\frac{{}_2\mathcal{F}_1(5/2,3/2;2;(b/2+\psi-\varphi)/(b/2+\psi+\varphi))}{(s+\psi+\varphi)^{5/2}}. \tag{27}$$

A generalized closed-form expression for the moments of the SNR can be obtained by substituting (25) into $\overline{\gamma_{\text{eq,ideal}}^n} = \int_0^\infty nx^{n-1}\overline{F}_{\gamma_{\text{eq,ideal}}}(x)\mathrm{d}x$ and evaluating the resulting integral as follows (Appendix G):

$$\overline{\gamma_{\text{eq,ideal}}^n} = \frac{8n\sqrt{\pi}}{\overline{\gamma}_1\overline{\gamma}_2\Delta(\mathbf{\Psi}_D)}\sum_{j=1}^{N_d}\sum_{l=1}^{N_r}\binom{N_r}{l}l(-1)^{j+l+N_d+1}\lambda_j^{N_d-2} \times\Delta_{Nd,j}(A(\mathbf{\Psi}_D)) \times\frac{{}_2\mathcal{F}_1(n+2,3/2;n+3/2;(\psi-\varphi)/(\psi+\varphi))}{(\psi+\varphi)^{n+2}}. \tag{28}$$

The SNR moments can be used to study the higher-order metrics, such as the skewness and the kurtosis that characterize the distribution of $\gamma_{\text{eq,ideal}}$. The skewness ($\mathcal{S}$), which is a measure of the symmetry of the distribution, can be obtained as $\mathcal{S} = \overline{\gamma_{\text{eq,ideal}}^3}/(\overline{\gamma_{\text{eq,ideal}}^2})^{3/2}$. The kurtosis ($\mathcal{K}$), which quantifies the degree of peakedness of the distribution, is given by $\mathcal{K} = \overline{\gamma_{\text{eq,ideal}}^4}/(\overline{\gamma_{\text{eq,ideal}}^2})^2$. On the other hand, the amount of fading (AoF) is a performance metric which quantifies the severity of the fading that the signal experienced from the source to the destination. The AoF is given by $\text{AoF} = \overline{\gamma_{\text{eq,ideal}}^2}/(\overline{\gamma}_{\text{eq,ideal}})^2 - 1$.

3.6. High SNR Analysis. This section presents the high SNR analyses for the proposed system model when the antennas at the relay are uncorrelated.

3.6.1. The Outage Probability at High SNR. The behavior of the cumulative distribution function (CDF) of γ_{eq} for large $\overline{\gamma}$ is equivalent to the behavior of $F_{\gamma_{\text{eq}}}(y)$ around $y = 0$ [39]. By substituting $\overline{\gamma}_1 = \overline{\gamma}_2 = \overline{\gamma}$ and $x = \overline{\gamma}y$ into (25) and by expressing the exponential function and the Bessel function in terms of their Taylor series expansions around $y = 0$ [38, equations (1.211) and (8.446)], one obtains the expression with the lowest powers of y. Now, by collecting the first-order terms, the high SNR approximation (i.e., when $\overline{\gamma} = \overline{\gamma}_1 = \overline{\gamma}_2 \to \infty$) for the CDF of the end-to-end SNR (24) can be derived as follows:

$$F_{\gamma_{\text{eq}}}^{\infty}(x) \approx \begin{cases} \Omega_1 \left(\dfrac{x}{\overline{\gamma}}\right)^{N_r} + o\left(\dfrac{x}{\overline{\gamma}}\right)^{N_r+1}, & N_r < N_d, \\ \Omega_2 \left(\dfrac{x}{\overline{\gamma}}\right)^{N_d} + o\left(\dfrac{x}{\overline{\gamma}}\right)^{N_d+1}, & N_r > N_d, \\ \Omega_3 \left(\dfrac{x}{\overline{\gamma}}\right)^{N} + o\left(\dfrac{x}{\overline{\gamma}}\right)^{N+1}, & N = N_r = N_d, \end{cases} \tag{29}$$

where

$$\Omega_1 = \frac{2}{\Delta(\boldsymbol{\Psi}_D)(N_r)!} \sum_{j=1}^{N_d} \sum_{l=1}^{N_r} \binom{N_r}{l} (-1)^{N_r+N_d+j+l+2} \times \lambda_j^{N_d-3/2} l^{N_r+1/2} \Delta_{N_d,j}(A(\boldsymbol{\Psi}_D)),$$

$$\Omega_2 = \frac{1}{(N_d)! \prod_{i=1}^{N_d} \lambda_i},$$

$$\Omega_3 = \frac{1}{N!} \left[\left(\prod_{i=1}^{N} \lambda_i \right)^{-1} + \frac{2}{\Delta(\boldsymbol{\Psi}_D)(N)!} \sum_{j=1}^{N} \sum_{l=1}^{N} \binom{N}{l} \times (-1)^{N+N+j+l+2} \lambda_j^{N-3/2} l^{N+1/2} \Delta_{N,j}(A(\boldsymbol{\Psi}_D)) \right]. \tag{30}$$

At high SNR, the outage probability can easily be obtained by substituting (29) into $P_{\text{out}} = F_{\gamma_{\text{eq}}}^{\infty}(\gamma_{\text{th}})$.

3.6.2. The Symbol Error Rate at High SNR. The average SER at high SNR can be derived by substituting (29) into $\overline{P}_e = (a/2)\sqrt{(b/2\pi)} \int_0^{\infty} x^{-1/2} e^{-bx/2} F_{\gamma_{\text{eq}}}^{\infty}(x) \mathrm{d}x$ as follows:

$$P_e^{\infty} \approx \begin{cases} \dfrac{\Omega_1 a 2^{N_r-1} \Gamma(N_r + 1/2)}{\sqrt{\pi} (b\overline{\gamma})^{N_r}} + o\left(\overline{\gamma}^{-(N_r+1)}\right), & N_r < N_d, \\ \dfrac{\Omega_2 a 2^{N_d-1} \Gamma(N_d + 1/2)}{\sqrt{\pi} (b\overline{\gamma})^{N_d}} + o\left(\overline{\gamma}^{-(N_d+1)}\right), & N_r > N_d, \\ \dfrac{\Omega_3 a 2^{N-1} \Gamma(N + 1/2)}{\sqrt{\pi} (b\overline{\gamma})^{N}} + o\left(\overline{\gamma}^{-(N+1)}\right), & N = N_r = N_d. \end{cases} \tag{31}$$

In the high SNR regime, the average SER can be represented by $P_e^{\infty} \approx [G_c \overline{\gamma}]^{-G_d}$, where G_d and G_c are referred to as the diversity gain and coding gain, respectively [39]. By using (31), G_d and G_c are given by

$$G_d = \min(N_r, N_d), \tag{32}$$

$$G_c = \begin{cases} \dfrac{1}{b} \left(\dfrac{\Omega_1 a 2^{N_r-1} \Gamma(N_r + 1/2)}{\sqrt{\pi}} \right)^{-1/N_r}, & N_r < N_d, \\ \dfrac{1}{b} \left(\dfrac{\Omega_2 a 2^{N_d-1} \Gamma(N_d + 1/2)}{\sqrt{\pi}} \right)^{-1/N_d}, & N_r > N_d, \\ \dfrac{1}{b} \left(\dfrac{\Omega_3 a 2^{N-1} \Gamma(N + 1/2)}{\sqrt{\pi}} \right)^{-1/N}, & N = N_r = N_d, \end{cases} \tag{33}$$

respectively.

Remark 1. The diversity order of the proposed system is given by $G_d = \min(N_r, N_d)$ (32). If a single-antenna relay is used, then $G_d = \min(1, N_d) = 1$ even though the destination is equipped with multiple antennas. Thus, our analysis shows that in order to retain MIMO diversity benefits for dual-hop relay networks with single-antenna sources, the relay should be equipped with multiple antennas.

Remark 2. In our proposed system model, the relay uses only one transmit antenna for forwarding the amplified signal to the destination. Since the relay is already equipped with multiple antennas, transmit antenna selection (TAS) can also be employed at the relay. If the transmit antenna, which maximizes the end-to-end SNR, is used at the relay, then the diversity order of the system can be written by following (32) as

$$G_d^{\text{TAS}} = \min(N_r, N_r N_d) = N_r. \tag{34}$$

Thus, the system with TAS guarantees a diversity order of N_r whereas the system without TAS provides a diversity order of $\min(N_r, N_d)$. Hence TAS improves the diversity benefits only when $N_r > N_d$. However, when $N_r \leq N_d$, the system with TAS achieves coding gains despite no diversity advantages.

4. Numerical Results

This section presents the numerical and the simulation results for the proposed dual-hop AF MIMO relaying with antenna correlation. Monte Carlo simulation results are provided to verify the accuracy of the analytical derivations presented in Section 3. In computing the Gauss-Laguerre approximation for the outage probability (13), average bit error rate (BER) (14), and ergodic capacity (15), we choose L to be 25 for $1 \leq \min(N_r, N_d) \leq 3$ and L to be 30 for $\min(N_r, N_d) > 3$.

4.1. Comparison of Semiarbitrary and Arbitrary Correlation Models for the $S \to R$ Channel. In Figure 2, the average BER of BPSK for the proposed dual-hop MIMO relay network is plotted by taking into account two correlation models; (i) semiarbitrary correlation (ii) arbitrary correlation for the $S \to R$ channels. For both these cases, the $R \to D$

channel is arbitrary correlated. The average BER curves for the former case are plotted by using our closed-form BER approximation (14), whereas the Monte Carlo simulation results are used for the latter case. Figure 2 reveals clearly that the semiarbitrary correlation model agrees well with the arbitrary correlation model for different antenna setups. Thus, our analytical results may well be used to obtain design insights for dual-hop MIMO AF relay networks over arbitrary correlated fading. Figure 2 also verifies that the maximum diversity order is given by the minimum number of antenna at the relay and destination; $G_d = \min(N_r, N_d)$. This fact can also be proved by applying the min-max cut from the $S \rightarrow R$ and from $R \rightarrow D$ [40]. The BER curve corresponding to $N_r = 1$, $N_d = 1$ represents the dual-hop relaying with single-antenna terminals. The proposed dual-hop relay network with multiple-antenna relay and destination provides a substantial BER performance gains compared to single-antenna relaying. Moreover, the exact agreement between the analytical curves and the Monte-Carlo simulation points verifies the accuracy of our analysis.

4.2. Impact of Spatial Correlation on the Average BER. In Figure 3, the impact of antenna correlation at both the relay and destination on the average BER of the BPSK is depicted. Three different correlation effects are obtained by changing l_d, $\overline{\rho}$, and σ^2. Since l_d is the relative antenna spacing between the adjacent antennas in the linear array measured in the number of wavelengths, and σ_d^2 is the angular spread at the destination, smaller values of l_d and σ_d^2 result in higher antenna correlation at the destination. Moreover, the amount of antenna correlation at the relay can also be changed by changing $\overline{\rho}$, where $\overline{\rho}$ is a $1 \times N_r$ vector containing the elements ρ_p and ρ_q of $S \rightarrow R$ semiarbitrary correlation matrix (1). Thus, three correlation scenarios are obtained as (a) high correlation, (b) medium correlation, and (c) low correlation. Figure 3 reveals clearly that the higher correlation effect at both the relay and destination degrades the BER performance significantly.

4.3. Impact of Spatial Correlation on the Outage Probability. In Figure 4, the outage probability is plotted against the correlation coefficient of the $S \rightarrow R$ channels for the low, medium, and high spatial correlation scenarios in the $R \rightarrow D$ channels. Here, the $S \rightarrow R$ channels undergo equally correlated fading. The outage probability performance significantly degrades as the correlation of antennas at the relay increases. Moreover, this figure also shows that the correlation of the antennas at the destination has a considerable impact on the outage probability.

4.4. Impact of Spatial Correlation on the Ergodic Capacity. Figure 5 shows the impact of spatial correlation of antenna elements at relay and the destination on the ergodic capacity for semiarbitrary correlated $S \rightarrow R$ and arbitrary correlated $R \rightarrow D$ channels. Lower antenna spacing (i.e., higher spatial correlation) results in substantial losses in capacity. Figure 5 also reveals that the smaller angular spreads (i.e., higher spatial correlation) degrade the capacity benefits. A

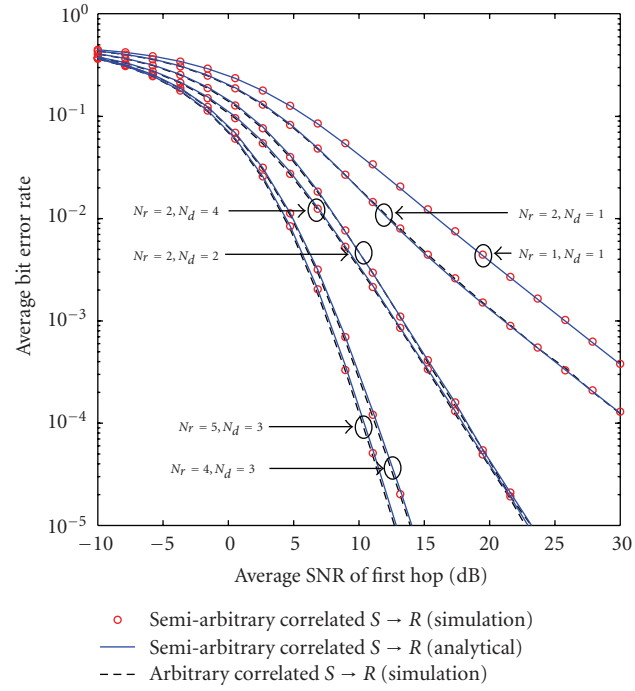

FIGURE 2: Average BER of BPSK for dual-hop MIMO relaying with antenna correlation at the relay and destination. $\overline{\gamma}_1 = \overline{\gamma}_2/2$. $l_s = l_d = 0.5$, $\theta_s = \theta_d = 3\pi/2$, and $\sigma_s^2 = \sigma_d^2 = \pi/6$. For $N_r = 2$, $N_r = 4$, and $N_r = 5$, $\overline{\rho}$ is chosen as $[0.5, 0.55]$, $[0.45, 0.55, 0.50, 0.60]$, and $[0.55, 0.50, 0.45, 0.65, 0.60]$, respectively.

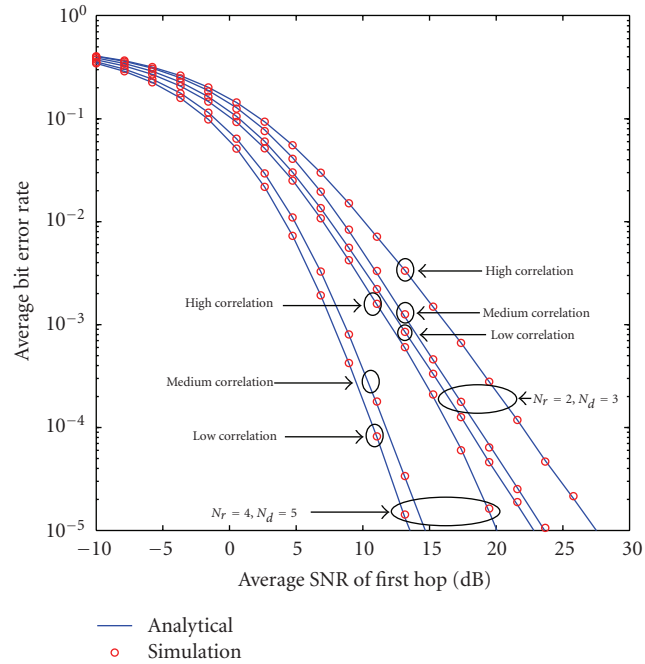

FIGURE 3: The impact of antenna correlation at the relay and destination on the average BER of BPSK. (a) High correlation: ($\overline{\rho}_h$, $l_d = 0.2$, $\sigma_d^2 = \pi/48$); (b) medium correlation: ($\overline{\rho}_m$, $l_d = 0.5$, $\sigma_d^2 = \pi/24$); (c) low correlation: ($\overline{\rho}_l$, $l_d = 0.8$, $\sigma_d^2 = \pi/6$). Here, $\overline{\rho}_{\mathbf{h}} = [0.8, 0.85]$, $\overline{\rho}_m = [0.55, 0.45]$, and $\overline{\rho}_l = [0.2, 0.3]$ for $N_r = 2$, and $\overline{\rho}_h = [0.8, 0.85, 0.75, 0.8]$, and $\overline{\rho}_m = [0.55, 0.45, 0.4, 0.5]$, $\overline{\rho}_l = [0.2, 0.3, 0.25, 0.35]$ for $N_r = 4$.

higher number of antennas at both the relay and destination increase the capacity benefits of dual-hop systems.

4.5. Sensitivity to the Antenna Spacing and Angular Spread. Figure 6 plots the average BER of BPSK against the antenna spacing for three different angular spreads ($\sigma_d^2 = \pi/6$, $\sigma_d^2 = \pi/12$, and $\sigma_d^2 = \pi/24$). Here, the $S \rightarrow R$ channel is equally correlated whereas the $R \rightarrow D$ channel is arbitrary correlated. Two different antenna configurations at the relay and destination are considered. Lower antenna spacings and angular spreads at the destination degrade the BER performance considerably. The BER curves seem to be approaching a fixed value once the antenna spacing is increased beyond 2.5 λ, regardless of the angular spread.

4.6. Numerical Results for the Special Cases. This section presents the numerical results for the special cases: (1) dual-antenna relay and (2) uncorrelated antennas at the relay.

4.6.1. Dual-Antenna Relay. In Figures 7 and 8, we analyze the tightness of the lower bounds developed for the average BER and the outage probability for the special case of dual-antenna relay. Both the lower bounds are tighter to the exact curves at moderate-to-high SNR regime. Thus, these bounds may serve as benchmarks for performance analysis of practical systems with practical CSI-assisted relays. In computing the lower bound for average BER by using the MGF approach, we choose N_p to be 10 for the Gauss-Chebyshev approximation in (22). The exact agreement between the BER curves evaluated using (22) and Monte Carlo simulation results validates the computational accuracy of our analysis.

Figures 7 and 8 also reveal that the average BER and the outage probability performance gap between the curves corresponding to high correlation and medium correlation are larger than those of curves corresponding to low correlation and medium correlation. The reason for this performance gap difference is because when $l_d > 0.38$ [32], the effect of antenna correlation at the destination becomes negligible, and the performance degradation is resulted solely by the antenna correlation at the relay. However, when $\rho = 0.9$, $l_d = 0.1$, the performance is degraded by antenna correlation at the relay and destination.

4.6.2. Uncorrelated Antennas at the Relay. In Figure 9, the outage probability of dual-hop MIMO relaying with uncorrelated antennas at the relay and correlated antennas at the destination is plotted against the destination angular spread. It shows that the outage probability degrades considerably due to the spatial correlation of antennas at the destination. Higher angular spreads degrade the outage probability performance significantly. Lowering the antenna spacing at the destination adversely impacts the outage probability.

Figure 10 shows the average BER performance of dual-hop MIMO relaying with uncorrelated antennas at the relay and correlated antennas at the destination. Figure 10 also shows the high SNR analysis of the average BER for different antenna configurations at the relay and destination. The analytical curves obtained from (27) agree exactly with

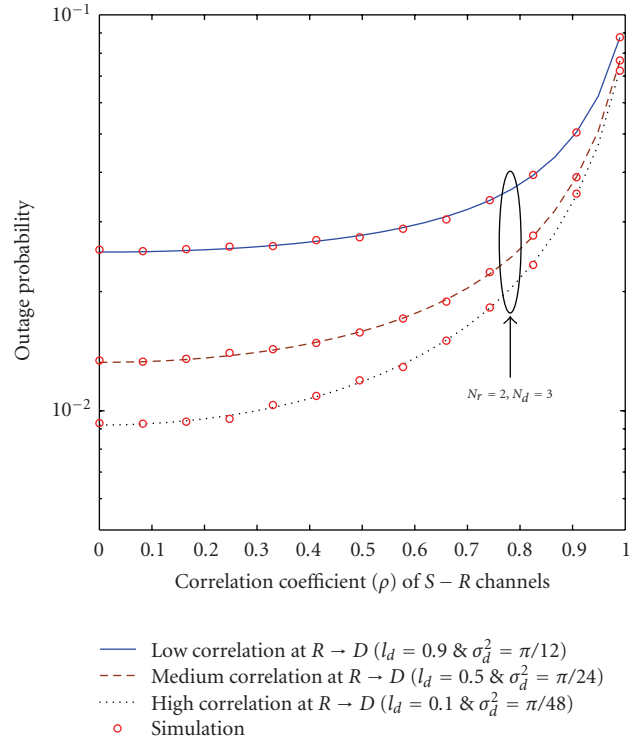

FIGURE 4: Impact of spatial correlation on the outage probability of dual-hop MIMO relaying. $\overline{\gamma}_1 = \overline{\gamma}_2/2 = 10$ dB and $\overline{\theta}_d = \pi/6$.

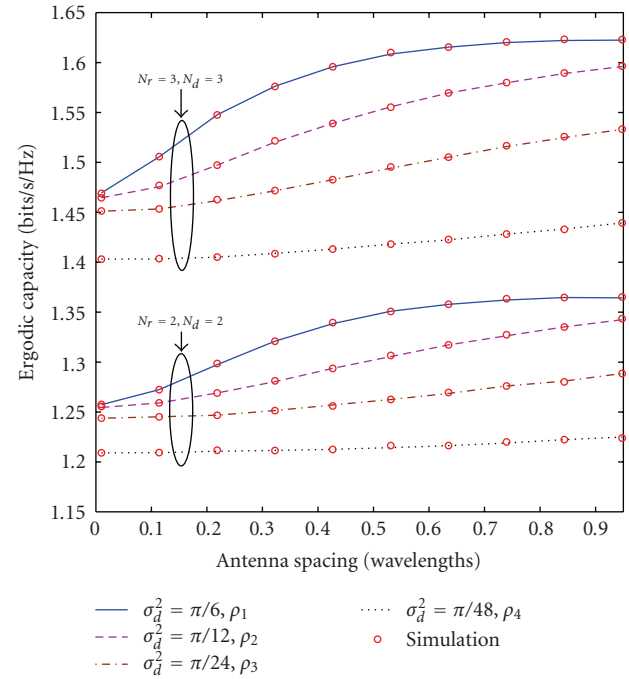

FIGURE 5: The impact of correlation coefficient of source-to-relay channels and antenna spacing/angular spread at the destination on the ergodic capacity. $\overline{\gamma}_1 = \overline{\gamma}_2/2 = 10$ dB. $\overline{\theta} = \pi/4$. For $N_r = 2$, the $S \rightarrow R$ semiarbitrary correlation matrix is parameterized by $\overline{\rho}_1 = [0.2, 0.25]$, $\overline{\rho}_2 = [0.4, 0.45]$, $\overline{\rho}_3 = [0.6, 0.65]$, and $\overline{\rho}_4 = [0.8, 0.85]$. For $N_r = 3$, $S \rightarrow R$ correlation matrix is parameterized by $\overline{\rho}_1 = [0.2, 0.25, 0.3]$, $\overline{\rho}_2 = [0.45, 0.5, 0.45]$, $\overline{\rho}_3 = [0.6, 0.65, 0.55]$, and $\overline{\rho}_4 = [0.85, 0.8, 0.75]$.

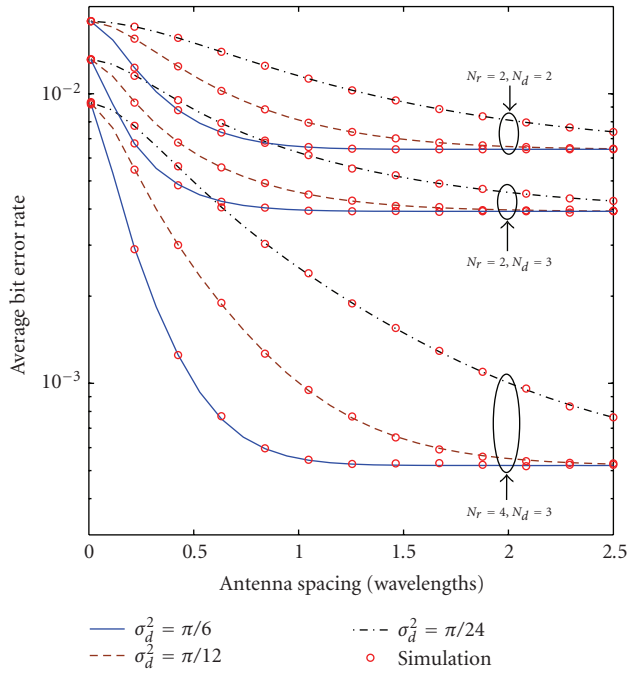

FIGURE 6: Impact of antenna spacing/angular spread at the destination on the average BER of BPSK. $\overline{\gamma}_1 = \overline{\gamma}_2 = 10\,\text{dB}$, $\rho = 0.5$, and $\overline{\theta}_d = \pi/6$.

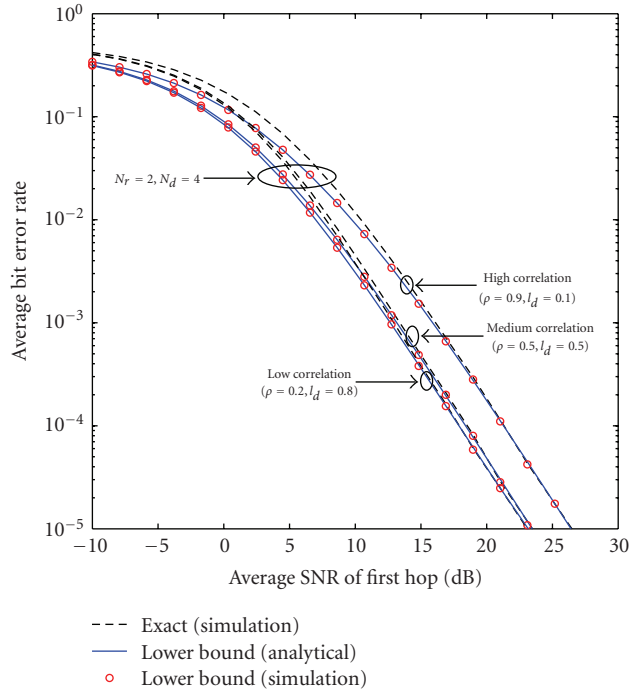

FIGURE 7: Average BER of dual-hop MIMO relaying over correlated Rayleigh fading channels with two antennas at the relay and four antennas at the destination. $\overline{\gamma}_1 = \overline{\gamma}_2/2$, $\overline{\theta}_d = \pi/6$, and $\sigma_d^2 = \pi/6$.

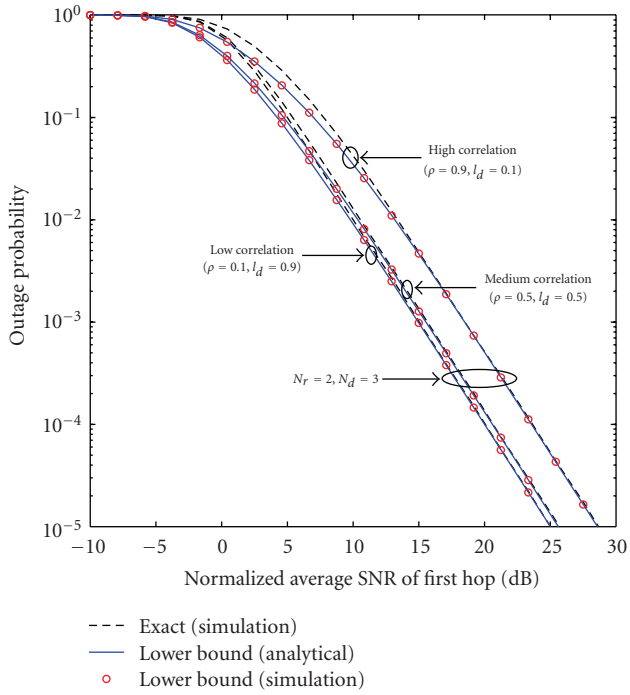

FIGURE 8: Outage probability of dual-hop MIMO relaying over correlated Rayleigh fading channels with two antennas at the relay and three antennas at the destination. $\overline{\gamma}_1 = \overline{\gamma}_2/2$, $\overline{\theta}_d = 3\pi/6$, and $\sigma_d^2 = \pi/6$.

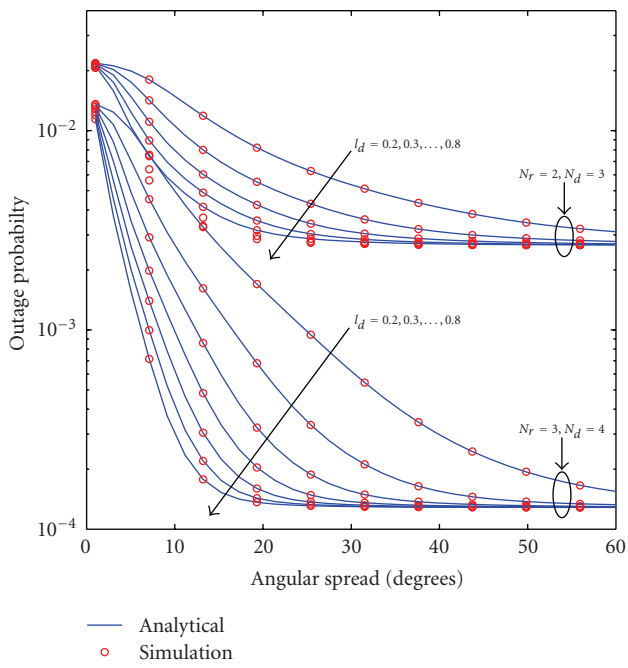

FIGURE 9: Impact of destination antenna angular spread on the outage probability of dual-hop MIMO relaying with uncorrelated antennas at the relay and correlated antennas at the destination. $\overline{\gamma}_1 = \overline{\gamma}_2/2 = 10\,\text{dB}$, $\rho = 0$, and $\overline{\theta}_d = \pi/6$.

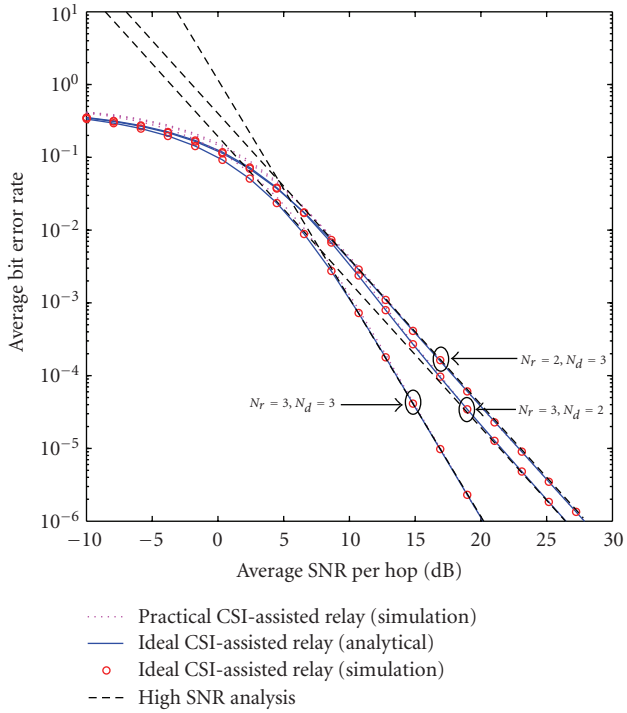

FIGURE 10: Average BER of dual-hop MIMO relaying over Rayleigh fading channels with uncorrelated antennas at the relay and correlated antennas at the destination. $\overline{\gamma}_1 = \overline{\gamma}_2$, $\rho = 0, \overline{\theta}_d = \pi/4$, $l_d = 0.6$, and $\sigma_d^2 = \pi/6$.

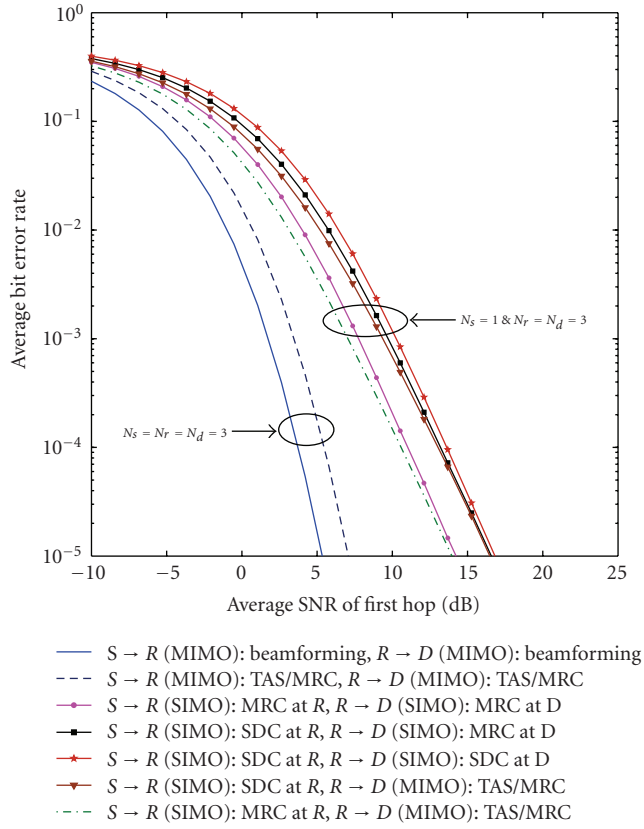

FIGURE 11: Average BER of several dual-hop MIMO AF relay system models over arbitrary correlated Rayleigh fading channels. $\overline{\gamma}_1 = \overline{\gamma}_2$, $\overline{\theta}_r = \overline{\theta}_d = \pi/4$, $l_r = l_d = 0.6$, and $\sigma_r^2 = \sigma_d^2 = \pi/6$.

the Monte Carlo simulation points. The average BER with ideal CSI-assisted relays serves as tight lower bounds or a benchmark for the average BER with practical CSI-assisted relays.

4.7. Comparison of BER of BPSK for Several Dual-Hop MIMO AF Relay System Models. Figure 11 compares the average BER of BPSK for several dual-hop MIMO AF relaying models over arbitrary correlated fading. These average BER curves are plotted by using Monte-Carlo simulation results. This figure shows that dual-hop relay networks, which use beamforming or TAS at $S \rightarrow R$ and $R \rightarrow D$ channels with MIMO channels (i.e., multiple antennas at each terminal) outperform the networks with SIMO channels (i.e., single-antenna source and the relay uses only a single transmit antenna out of N_r in the second timeslot). Further, it shows that although the TAS is performed at the relay for the $R \rightarrow D$ channel, no diversity gains but a coding gain can be achieved over the use of arbitrary single transmit antenna when $N_r = N_d$. For dual-hop relay models, which use SDC with SIMO channels for $S \rightarrow R$ and $R \rightarrow D$, perform relatively well with those which use MRC. Although the proposed model (see BER curve corresponding to [$S \rightarrow R$ (SIMO): SDC at R, $R \rightarrow D$ (SIMO): MRC at D] in Figure 11) is suboptimal, it achieves most of the MIMO benefits while using only one transmit/receive chain at the relay.

5. Conclusion

A suboptimal yet simple and realistic dual-hop AF MIMO relay network model was developed. The impact of spatial correlation on the performance of the proposed system model over Rayleigh fading was investigated by using a semiarbitrary and arbitrary correlation models for the $S \rightarrow R$ and $R \rightarrow D$ channels, respectively. Accurate closed-form expressions for the CCDF, the MGF, the outage probability, the average symbol error rate, and the ergodic capacity were derived. The performance of two special cases was studied: (1) dual-antenna relay and multiple-antenna destination, and (2) uncorrelated antennas at the relay and correlated antennas at the destination. The high SNR approximations for the outage probability and the average were derived to obtain valuable system design insights such as the diversity order and coding gain. Numerical and Monte Carlo simulation results were presented to investigate the detrimental effect of the antenna correlation on the system performance and to validate our analyses. Our results show that in order to retain MIMO benefits for dual-hop relay networks that consist of single-antenna sources and multiple-antenna destinations, MIMO-enabled relays should be used. Our results may be useful in analyzing practical system scenarios that involve a single-antenna portable device communicating

with a multiple-antenna base station via an infrastructure-based fixed relay equipped with multiple antennas.

Appendices

This section provides sketches of the proofs of some of the results presented in Section 3.

A. Statistical Characterization of the End-to-End SNR

The closed-form approximation for the CCDF of the end-to-end SNR in (8) can be obtained by using the following integral expression [13]:

$$\overline{F}_{\gamma_{\text{eq}}}(x) = \int_0^\infty \overline{F}_{\gamma_1}\left(\frac{(z+x+1)x}{z}\right) f_{\gamma_2}(z+x)\mathrm{d}z, \tag{A.1}$$

where $\overline{F}_{\gamma_1}(x)$ and $f_{\gamma_2}(x)$ are the CCDF and probability density function (PDF) of γ_1 and γ_2, respectively. The CCDF of γ_1 can be written as in [27, 36]

$$\overline{F}_{\gamma_1}(x) = 1 - \int_0^\infty \prod_{k=1}^{N_r}\left[1 - \mathcal{Q}\left(\sqrt{\frac{2\rho_k t}{1-\rho_k}}, \sqrt{\frac{2y}{\overline{\gamma}_1(1-\rho_k)}}\right)\right] e^{-t}\mathrm{d}t. \tag{A.2}$$

The PDF of γ_2 can be written as in [10]

$$f_{\gamma_2}(x) = \sum_{j=1}^{N_d} \frac{(-1)^{j+N_d}}{\overline{\gamma}_2 \Delta(\mathbf{\Psi}_D)} \lambda_j^{N_d-2} \Delta_{N_d,j}(A(\mathbf{\Psi}_D)) e^{-x/\overline{\gamma}_2\lambda_j}, \tag{A.3}$$

where λ_j, $\mathbf{\Psi}_D$, $\Delta(\mathbf{\Psi}_D)$, $\Delta_{N_d,j}(\mathcal{M})$, and $A(\mathcal{M})$ are defined in (11). By substituting (A.2) and (A.3) into (A.1), we obtain an integral expression for the CCDF of the SNR as follows:

$$\overline{F}_{\gamma_{\text{eq}}}(x) = \frac{1}{\Delta(\mathbf{\Psi}_D)} \sum_{j=1}^{N_d} (-1)^{N_d+j} \lambda_j^{N_d-1} \Delta_{N_d,j}(A(\mathbf{\Psi}_D)) e^{-x/\overline{\gamma}_2\lambda_j} \times \left(1 - \iint_0^\infty \prod_{k=1}^{N_r} [1 - \mathcal{Q}(\Upsilon_1(t), \Upsilon_2(t,y))] e^{-(y+t)}\mathrm{d}y\,\mathrm{d}t\right), \tag{A.4}$$

where $\Upsilon_1(t) = \sqrt{2\rho_k t/(1-\rho_k)}$ and $\Upsilon_2(t,y) = \sqrt{2x(x+\overline{\gamma}_2\lambda_j y+1)/\overline{\gamma}_1\overline{\gamma}_2\lambda_j(1-\rho_k)y}$. No closed-form solution for the double-integral (A.4) appears to be available. However, it is in the form of $\iint_0^\infty f(x,y)e^{-x}e^{-y}\mathrm{d}x\,\mathrm{d}y$, and, thus, it can be efficiently and accurately approximated by using the Gauss-Laguerre quadrature rule [23] in closed form as in (11).

The MGF of γ_{eq} can be derived as follows:

$$M_{\gamma_{\text{eq}}}(s) = \int_0^\infty f_{\gamma_{\text{eq}}}(x)e^{-sx}\mathrm{d}x = 1 - \int_0^\infty s\overline{F}_{\gamma_{\text{eq}}}(x)e^{-sx}\mathrm{d}x. \tag{A.5}$$

The second equality of (A.5) is obtained by integrating by parts and considering that $f_{\gamma_{\text{eq}}}(x) = 0, \forall x \le 0$. By substituting (A.4) into (A.5), the MGF of γ_{eq} is obtained as follows:

$$M_{\gamma_{\text{eq}}}(s) = 1 - \sum_{j=1}^{N_d} \frac{(-1)^{N_d+j}}{\Delta(\mathbf{\Psi}_D)} \lambda_j^{N_d} \Delta_{N_d,j}(A(\mathbf{\Psi}_D)) \frac{s}{\lambda_j s + 1/\overline{\gamma}_2} \times \left(1 - \iiint_0^\infty \prod_{k=1}^{N_r}\left[1 - \mathcal{Q}\left(\sqrt{\alpha_k}, \sqrt{\beta_k}\right)\right] e^{-(y+z+t)}\mathrm{d}y\,\mathrm{d}z\,\mathrm{d}t\right), \tag{A.6}$$

where $\alpha_k = 2\rho_k t/(1-\rho_k)$ and $\beta_k = 2\overline{z}(\overline{\gamma}_2\lambda_j z + (1+\overline{\gamma}_2\lambda_j y)(1+\overline{\gamma}_2\lambda_j s))/\overline{\gamma}_1(1+\overline{\gamma}_2\lambda_j s)^2(1-\rho_k)y$. Again, one can accurately approximate $M_{\gamma_{\text{eq}}}(s)$ in (A.6) by using the Gauss-Laguerre quadrature rule as in (12).

B. Average Symbol Error Rate

The average SER has the integral representation [31]

$$\overline{P}_e = \mathcal{E}_{\gamma_{\text{eq}}}\{P_e \mid \gamma\} = \frac{a}{2} - \frac{a}{2}\sqrt{\frac{b}{2\pi}} \int_0^\infty x^{-1/2} e^{-bx/2} \overline{F}_{\gamma_{\text{eq}}}(x)\mathrm{d}x. \tag{B.1}$$

By substituting (A.4) into (B.1), the average SER is obtained as follows:

$$\overline{P}_e = \frac{a}{2} - \frac{a}{2\Delta(\mathbf{\Psi}_D)}\sqrt{\frac{b}{2}} \sum_{j=1}^{N_d} (-1)^{N_d+j} \lambda_j^{N_d-1} \Delta_{N_d,j}(A(\mathbf{\Psi}_D)) \times \sqrt{\frac{2}{b+2/\overline{\gamma}_2\lambda_j}} \left(1 - \frac{1}{\sqrt{\pi}} \iiint_0^\infty z^{-1/2} \times \prod_{k=1}^{N_r}\left[1 - \mathcal{Q}\left(\sqrt{\alpha_k}, \sqrt{\zeta_k}\right)\right] e^{-(y+z+t)}\mathrm{d}y\mathrm{d}z\mathrm{d}t\right), \tag{B.2}$$

where $\alpha_k = 2\rho_k t/(1-\rho_k)$ and $\zeta_k = 4z(2\overline{\gamma}_2\lambda_j z + (1+\overline{\gamma}_2\lambda_j y)(2+b\overline{\gamma}_2\lambda_j))/\overline{\gamma}_1(2+b\overline{\gamma}_2\lambda_j)^2(1-\rho_k)y$. Since the triple integral (B.2) does not appear amenable to a closed-form solution, we again use the Gauss-Laguerre quadrature rule to obtain an accurate average SER approximation as in (14).

C. MGF of the Upper Bounded SNR with Two Receive Antennas at the Relay

By substituting (19) into (A.5), one gets

$$M_{\gamma_{\text{eq}}^{\text{ub}}}(s) = 1 - \frac{s}{\Delta(\mathbf{\Psi}_D)} \sum_{j=1}^{N_d} 2(-1)^{j+N_d} \lambda_j^{N_d-1} \times \Delta_{Nd,j}(A(\mathbf{\Psi}_D))(I_1 + I_2), \tag{C.1}$$

where

$$I_1=\int_0^\infty 2e^{-x((\overline{\gamma}_1+\overline{\gamma}_2\lambda_j)/\overline{\gamma}_1\overline{\gamma}_2\lambda_j+s)}\mathcal{Q}\left(\sqrt{\frac{2x}{\overline{\gamma}_1(1-\rho^2)}},\rho\sqrt{\frac{2x}{\overline{\gamma}_1(1-\rho^2)}}\right)\mathrm{d}x$$

$$I_2=\int_0^\infty e^{-x((\overline{\gamma}_1(1-\rho^2)+2\overline{\gamma}_2\lambda_j)/\overline{\gamma}_1\overline{\gamma}_2\lambda_j(1-\rho^2)+s)}I_0\left(\frac{2\rho x}{\overline{\gamma}_1(1-\rho^2)}\right)\mathrm{d}x. \tag{C.2}$$

The integral I_1 can be solved by substituting $x=y^2$ and by using [41, equations (55) and (56)] as $I_1=(1/(s+\mu))(1+(s+\mu+1/\overline{\gamma})/\sqrt{(s+\mu+\varepsilon)^2-\varsigma^2})$, where $\mu=(\overline{\gamma}_1+\overline{\gamma}_2\lambda_j)/\overline{\gamma}_1\overline{\gamma}_2\lambda_j$, $\varepsilon=(1+\rho^2)/\overline{\gamma}_1(1-\rho^2)$, and $\varsigma=2\rho/\overline{\gamma}_1(1-\rho^2)$. The integral I_2 can be solved by using [42, 4.16.6] as $I_2=1/\sqrt{(s+\nu)^2-\varsigma^2}$, where $\nu=(\overline{\gamma}_1(1-\rho^2)+2\overline{\gamma}_2\lambda_j)/\overline{\gamma}_1\overline{\gamma}_2\lambda_j(1-\rho^2)$. Substitution of I_1 and I_2 into (C.1) yields the desired result given in (20).

D. CCDF of SNR with Uncorrelated Antennas at the Relay

When the $S\rightarrow R$ channel undergoes independent Rayleigh fading, one can obtain the CCDF of γ_{eq} by letting $\rho=0$ in (A.4) as $\overline{F}_{\gamma_{\mathrm{eq}}}(x)=(1/\Delta(\mathbf{\Psi}_D))\sum_{j=1}^{N_d}(-1)^{N_d+j}\lambda_j^{N_d-1}\Delta_{N_d,j}(A(\mathbf{\Psi}_D))e^{-x/\overline{\gamma}_2\lambda_j}(1-I_3)$, where $I_3=\iint_0^\infty[1-\mathcal{Q}(0,\sqrt{2x(x+\overline{\gamma}_2\lambda_j y+1)/\overline{\gamma}_1\overline{\gamma}_2\lambda_j y)}]^{N_r}\times e^{-(y+t)}\mathrm{d}y\,\mathrm{d}t$. By using the fact that $\mathcal{Q}(0,b)=e^{-b/2}$ [41, equation (2)] and binomial expansion, I_3 can be simplified to the following form:

$$I_3=1+\sum_{l=1}^{N_r}\binom{N_r}{l}(-1)^l e^{-xl/\overline{\gamma}_1}\int_0^\infty e^{-(xl(x+1)/\overline{\gamma}_1\overline{\gamma}_2\lambda_j y+y)}\mathrm{d}y. \tag{D.1}$$

By evaluating the integral in (D.1) by using [25, 3.471.9], one can obtain the result given in (25).

E. MGF of the SNR with Uncorrelated Antennas at an Ideal CSI-Assisted Relay

By substituting the CCDF of the SNR given in (25) into (A.5), one obtains

$$M_{\gamma_{\mathrm{eq,ideal}}}(s)=1-\frac{2s}{\Delta(\mathbf{\Psi}_D)}\sum_{j=1}^{N_d}\sum_{l=1}^{N_r}\binom{N_r}{l}(-1)^{N_d+j+l+1}\lambda_j^{N_d-1}\times\Delta_{N_d,j}(A(\mathbf{\Psi}_D))\sqrt{\frac{l}{\overline{\gamma}_1\overline{\gamma}_2\lambda_j}}I_4, \tag{E.1}$$

where $I_4=\int_0^\infty xe^{-((\overline{\gamma}_1+\overline{\gamma}_2\lambda_j l)/\overline{\gamma}_1\overline{\gamma}_2\lambda_j+s)}\mathcal{K}_1(2x\sqrt{l/\overline{\gamma}_1\overline{\gamma}_2\lambda_j})\mathrm{d}x$. The integral I_4 can be evaluated by using [25, 6.621.3] to yield the desired result given in (26).

F. Average SER with Uncorrelated Antennas at an Ideal CSI-Assisted Relay

By substituting (25) into (B.1), one obtains the following:

$$\overline{P}_e=\frac{a}{2}-\frac{a}{\Delta(\mathbf{\Psi}_D)}\sqrt{\frac{b}{2\pi}}\sum_{j=1}^{N_d}\sum_{l=1}^{N_r}(-1)^{N_d+j+l+1}\lambda_j^{N_d-1}\times\Delta_{N_d,j}(A(\mathbf{\Psi}_D))\sqrt{\frac{l}{\overline{\gamma}_1\overline{\gamma}_2\lambda_j}}I_5, \tag{F.1}$$

where $I_5=\int_0^\infty x^{-1/2}e^{-x(b/2+(\overline{\gamma}_1+\overline{\gamma}_2\lambda_j l)/\overline{\gamma}_1\overline{\gamma}_2\lambda_j)}\mathcal{K}_1(2x\sqrt{l/\overline{\gamma}_1\overline{\gamma}_2\lambda_j})\mathrm{d}x$. We solve I_5 by using [25, 6.621.3], and substituting into (F.1), we obtain the desired result given in (27).

G. Moments of SNR with Uncorrelated Antennas at an Ideal CSI-Assisted Relay

By substituting (25) into $\overline{\gamma_{\mathrm{eq,ideal}}^n}=\int_0^\infty nx^{n-1}\overline{F}_{\gamma_{\mathrm{eq,ideal}}}(x)\mathrm{d}x$, one obtains

$$\overline{\gamma_{\mathrm{eq,ideal}}^n}=\frac{2n}{\Delta(\mathbf{\Psi}_D)}\sum_{j=1}^{N_d}\sum_{l=1}^{N_r}\binom{N_r}{l}(-1)^{j+l+N_d+1}\lambda_j^{N_d-1}\times\Delta_{Nd,j}(A(\mathbf{\Psi}_D))\sqrt{\frac{l}{\overline{\gamma}_1\overline{\gamma}_2\lambda_j}}I_6, \tag{G.1}$$

where $I_6=\int_0^\infty x^n e^{-x((\overline{\gamma}_1+\overline{\gamma}_2\lambda_j l)/\overline{\gamma}_1\overline{\gamma}_2\lambda_j)}\mathcal{K}_1(2x\sqrt{l/\overline{\gamma}_1\overline{\gamma}_2\lambda_j})\mathrm{d}x$. The desired result in (28) can be obtained by solving I_6 by using [25, 6.621.3].

References

[1] J. N. Laneman, D. N. C. Tse, and G. W. Wornell, "Cooperative diversity in wireless networks: efficient protocols and outage behavior," *IEEE Transactions on Information Theory*, vol. 50, no. 12, pp. 3062–3080, 2004.

[2] R. Pabst, B. H. Walke, D. C. Schultz et al., "Relay-based deployment concepts for wireless and mobile broadband radio," *IEEE Communications Magazine*, vol. 42, no. 9, pp. 80–89, 2004.

[3] H. Yanikomeroglu, "Fixed and mobile relaying technologies for cellular networks," in *Proceedings of the 2nd Workshop on Applications and Services in Wireless Networks (ASWN '02)*, pp. 75–81, July 2002.

[4] M. O. Hasna and M.-S. Alouini, "End-to-end performance of transmission systems with relays over Rayleigh-fading channels," *IEEE Transactions on Wireless Communications*, vol. 2, no. 6, pp. 1126–1131, 2003.

[5] P. A. Anghel and M. Kaveh, "Exact symbol error probability of a cooperative network in a rayleigh-fading environment," *IEEE Transactions on Wireless Communications*, vol. 3, no. 5, pp. 1416–1421, 2004.

[6] A. Adinoyi and H. Yanikomeroglu, "Cooperative relaying in multi-antenna fixed relay networks," *IEEE Transactions on Wireless Communications*, vol. 6, no. 2, pp. 533–544, 2007.

[7] Y. Kim and H. Liu, "Infrastructure relay transmission with cooperative MIMO," *IEEE Transactions on Vehicular Technology*, vol. 57, no. 4, pp. 2180–2188, 2008.

[8] Ö. Oyman, J. N. Laneman, and S. Sandhu, "Multihop relaying for broadband wireless mesh networks: from theory to practice," *IEEE Communications Magazine*, vol. 45, no. 11, pp. 116–122, 2007.

[9] Y. Fan and J. Thompson, "MIMO configurations for relay channels: Theory and practice," *IEEE Transactions on Wireless Communications*, vol. 6, no. 5, pp. 1774–1786, 2007.

[10] R. H. Louie, Y. Li, H. A. Suraweera, and B. Vucetic, "Performance analysis of beamforming in two hop amplify and forward relay networks with antenna correlation," *IEEE Transactions on Wireless Communications*, vol. 8, no. 6, pp. 3132–3141, 2009.

[11] D. B. Da Costa and S. Aissa, "Cooperative dual-hop relaying systems with beamforming over nakagami-m fading channels," *IEEE Transactions on Wireless Communications*, vol. 8, no. 8, pp. 3950–3954, 2009.

[12] S. Chen, W. Wang, X. Zhang, and D. Zhao, "Performance of amplify-and-forward MIMO relay channels with transmit antenna selection and maximal-ratio combining," in *Proceedings of IEEE Wireless Communications and Networking Conference (WCNC '09)*, April 2009.

[13] R. H. Y. Louie, Y. Li, and B. Vucetic, "Performance analysis of beamforming in two hop amplify and forward relay networks," in *Proceedings of IEEE International Conference on Communications (ICC '08)*, pp. 4311–4315, May 2008.

[14] H. Muhaidat and M. Uysal, "Cooperative diversity with multiple-antenna nodes in fading relay channels," *IEEE Transactions on Wireless Communications*, vol. 7, no. 8, pp. 3036–3046, 2008.

[15] A. Talebi and W. A. Krzymień, "Multiple-antenna multiple-relay cooperative communication system with beamforming," in *Proceedings of the 67th IEEE Vehicular Technology Conference (VTC '08)*, pp. 2350–2354, May 2008.

[16] P. Dharmawansa, M. R. McKay, and R. K. Mallik, "Dual hop MIMO relaying with orthogonal space-time block codes," in *Proceedings of IEEE International Conference on Communications (ICC '09)*, June 2009.

[17] B. K. Chalise and L. Vandendorpe, "Outage probability analysis of a MIMO relay channel with orthogonal space-time block codes," *IEEE Communications Letters*, vol. 12, no. 4, pp. 280–282, 2008.

[18] S. Ikki and M. H. Ahmed, "Performance analysis of cooperative diversity wireless networks over Nakagami-m fading channel," *IEEE Communications Letters*, vol. 11, no. 4, pp. 334–336, 2007.

[19] D. Senaratne and C. Tellambura, "Unified performance analysis of two hop amplify and forward relaying," in *Proceedings of IEEE International Conference on Communications*, Dresden, Germany, June 2009.

[20] S. Ikki and M. H. Ahmed, "Performance analysis of dual-hop relaying communications over generalized gamma fading channels," in *Proceedings of the 50th Annual IEEE Global Telecommunications Conference (GLOBECOM '07)*, pp. 3888–3893, November 2007.

[21] H. A. Suraweera, R. H. Y. Louie, Y. Li, G. K. Karagiannidis, and B. Vucetic, "Two hop amplify-and-forward transmission in mixed Rayleigh and Rician fading channels," *IEEE Communications Letters*, vol. 13, no. 4, pp. 227–229, 2009.

[22] S. S. Ikki and M. H. Ahmed, "Performance analysis of dual hop relaying over non-identical weibull fading channelsw," in *Proceedings of the 69th IEEE Vehicular Technology Conference (VTC '09)*, April 2009.

[23] M. Abramowitz and I. Stegun, *Handbook of Mathematical Functions*, Dover, New York, NY, USA, 1970.

[24] A. H. Nuttall, "Some integrals involving the QM-function," Tech. Rep., Naval Underwater Systems Center, New London Lab., May 1974.

[25] I. Gradshteyn and I. Ryzhik, *Table of Integrals, Series, and Products*, Academic Press, San Diego, Calif, USA, 7th edition, 2007.

[26] Q. T. Zhang and H. G. Lu, "A general analytical approach to multi-branch selection combining over various spatially correlated fading channels," *IEEE Transactions on Communications*, vol. 50, no. 7, pp. 1066–1073, 2002.

[27] X. Zhang and N. C. Beaulieu, "Performance analysis of generalized selection combining in generalized correlated Nakagami-m fading," *IEEE Transactions on Communications*, vol. 54, no. 11, pp. 2103–2112, 2006.

[28] Y. L. Tong, *The Multivariate Normal Distribution*, Spring, New York, NY, USA, 3rd edition, 1990.

[29] Q. T. Zhang, "Maximal-ratio combining over Nakagami fading channels with an arbitrary branch covariance matrix," *IEEE Transactions on Vehicular Technology*, vol. 48, no. 4, pp. 1141–1150, 1999.

[30] H. Bölcskei, M. Borgmann, and A. J. Paulraj, "Impact of the propagation environment on the performance of space-frequency coded MIMO-OFDM," *IEEE Journal on Selected Areas in Communications*, vol. 21, no. 3, pp. 427–439, 2003.

[31] M. R. McKay, A. J. Grant, and I. B. Collings, "Performance analysis of MIMO-MRC in double-correlated Rayleigh environments," *IEEE Transactions on Communications*, vol. 55, no. 3, pp. 497–507, 2007.

[32] J. Proakis, *Digital Communications*, McGraw-Hill, New York, NY, USA, 4th edition, 2001.

[33] G. H. Golub, et al., "Calculation of Gauss quadrature rules," Tech. Rep., Stanford University, Stanford, Calif, USA, 1967.

[34] H. A. David, *Order Statistics*, John Wiley & Sons, New York, NY, USA, 1981.

[35] H. Schwartz, W. Bennett, and S. Stein, *Communication Systems and Techniques*, McGraw-Hill, New York, NY, USA, 1966.

[36] Y. Chen and C. Tellambura, "Distribution functions of selection combiner output in equally correlated Rayleigh, Rician, and Nakagami-m fading channels," *IEEE Transactions on Communications*, vol. 52, no. 11, pp. 1948–1956, 2004.

[37] A. Annamalai, C. Tellambura, and V. K. Bhargava, "Efficient computation of MRC diversity performance in Nakagami fading channel with arbitrary parameters," *Electronics Letters*, vol. 34, no. 12, pp. 1189–1190, 1998.

[38] I. Gradshteyn and I. Ryzhik, *Table of Integrals, Series, and Products*, Academic Press, San Diego, Calif, USA, 6th edition, 2000.

[39] Z. Wang and G. B. Giannakis, "A simple and general parameterization quantifying performance in fading channels," *IEEE Transactions on Communications*, vol. 51, no. 8, pp. 1389–1398, 2003.

[40] M. Yuksel and E. Erkip, "Multiple-antenna cooperative wireless systems: a diversity-multiplexing tradeoff perspective," *IEEE Transactions on Information Theory*, vol. 53, no. 10, pp. 3371–3393, 2007.

[41] A. H. Nuttall, "Some integrals involving the Q-function," Tech. Rep., Naval Underwater Systems Center, New London Lab., 1972.

[42] A. Erdelyi, W. Magnus, and F. G. Tricomi, *Tables of Integral Transforms*, vol. 1, Mcgraw-Hill, New York, NY, USA, 1954.